MINISTRY OF EDUCATION
POLITEHNICA National University
of Science and Technology

Bucharest Doctoral
School of
Industrial Engineering
and Robotics

Cosmina Gh. CHIUJDEA

DOCTORAL THESIS

Study of the triboelectric behavior of 3D-printed polymeric surfaces

Scientific coordinator :
Prof.dr.ing. Sorin Cănănău

- 2025 -

Cuprins

Introduction ..... - 2 -
Part I. Current state of research in the field ..... - 4 -
Chapter 1. Additive Manufacturing ..... - 4 -
1.1. What is additive manufacturing? ..... - 4 -
1.2. The Main Stages in the Additive Manufacturing Process ..... - 5 -
Fields of application ..... - 6 -
1.3. Advantages and disadvantages ..... - 6 -
1.3.1. Advantages ..... - 6 -
1.4.2. Dezvantaje ..... - 7 -
1.4. Clasificare ..... - 8 -
Capitolul 2. Tribostatica ..... - 10 -
2.1. Stadiul actual al cercetării ..... - 10 -
2.2. Încărcarea prin efect triboelectric ..... - 11 -
Capitolul 3. Concluzii privind stadiul actual al cercetărilor în domeniu ..... - 12 -
Partea a II-a. Contribuții la studiul comportamentului triboelectric al suprafeţelor polimerice obţinute prin imprimare 3D ..... - 12 -
Capitolul 4. Direcţiile, obiectivul principal şi metodologia de cercetare-dezvoltare ..... - 12 -
4.1. Direcţii de cercetare-dezvoltare ..... - 12 -
4.2. Obiectivul principal al activităţii de cercetare-dezvoltare ..... - 13 -
4.3. Metodologia de cercetare-dezvoltare ..... - 13 -
4.4. Materiale și metode ..... - 14 -
4.5. Rezultate și discuții ..... - 20 -
4. Concluzii ..... - 23 -
Capitolul 5. Concluzii finale şi contribuţii principale ..... - 24 -
5.1. Concluzii finale ..... - 24 -
5.2. Contribuții principale ..... - 24 -
5.3. Importanța tezei ..... - 24 -
5.4. Perspective viitoare ..... - 25 -
Bibliografie ..... - 26 -

Introduction

In recent decades, additive manufacturing (AM) technologies have experienced remarkable development, being regarded as next-generation solutions for numerous challenges of modern industry. These technologies address fundamental requirements of today's economic environment: reducing production costs and lead times, enabling the fabrication of complex geometries, ensuring high process flexibility, and contributing to sustainability through efficient use of materials. At the same time, AM facilitates product customization and the rapid integration of innovations into the manufacturing cycle, strengthening its role in the transition toward Industry 4.0.

Nevertheless, the large-scale adoption of AM technologies still faces several technical and scientific challenges, including limitations in the range of available materials, high equipment costs, and the quality of the resulting surfaces. Among these, surface quality is a critical factor, directly influencing both dimensional accuracy and the functional performance of the manufactured products.

In parallel, interest in the use of polymers for energy and electrostatic applications has grown significantly. Materials such as PLA, due to their sustainable and biodegradable nature, represent an attractive option for the development of devices based on the triboelectric effect, such as triboelectric nanogenerators (TENGs). In this context, the surface texture of the material plays a decisive role in the tribo-charging process, affecting both the level and distribution of the generated electric charge.

Therefore, the necessity and importance of this thesis lie in its interdisciplinary approach to two emerging fields—additive manufacturing and triboelectricity—through the investigation of how 3D-printed surface texturing influences the tribo-charging process. The results obtained can contribute both to the optimization of AM processes and to the development of innovative applications in the fields of energy and self-powered devices.

The thesis is structured into several chapters, following a progressive logic from theoretical foundations to experimental results and conclusions:

- Chapter 1 – General aspects of additive manufacturing technologies – presents the evolution, classification, and fields of application of AM technologies, as well as their advantages and limitations.
- Chapter 2 – Surface quality in AM and its role in industrial applications – analyzes the factors influencing surface morphology and their impact on functional performance.

- Chapter 3 – Current state of research on triboelectrostatic phenomena – synthesizes the literature regarding the triboelectric effect, triboelectric nanogenerators, and the role of surface texturing.
- Chapter 4 – Research directions, main objective, and methodology – formulates the current research directions, defines the main objective of the thesis, and describes the methodology proposed to achieve it.
- Chapter 5 – Experimental results and their interpretation – presents in detail the investigations performed on 3D-printed polymer samples, focusing on the influence of surface texturing on the tribo-charging process, the comparative analysis of different texture types, and the discussion of the obtained results.

Part I. Current state of research in the field

Chapter 1. Additive Manufacturing

1.1. What is additive manufacturing?

Over time, companies have given priority to managing material, financial, technological, and human resources. Whereas in the past the main focus was on strict control of costs, raw materials, and equipment, today—in a highly globalized and extremely competitive environment—organizations recognize the crucial importance of additional factors. These include product quality, price competitiveness, delivery speed and reliability, process flexibility, and the ability to maintain a steady pace of innovation. Thus, competitive advantage is no longer defined solely by available resources but also by the capacity to implement advanced technologies and respond promptly to market demands.

The adoption of modern technologies in production processes generates a series of beneficial effects, among which the following stand out:

- Increased precision in execution and its consistency throughout the entire process, facilitating manufacturing optimization and the achievement of high-quality products;
- A higher degree of automation and digitalization of production lines, enabling real-time monitoring of technological parameters and rapid intervention in case of deviations;
- Improved labor productivity, both through reduced downtime and more efficient use of human and material resources;
- A steady increase in the quality of industrial products, strengthening customer trust and supporting access to demanding international markets.

As an essential component of the production process, the manufacturing system encompasses all activities through which raw material is transformed into a finished product or an intermediate product to be used in other stages of the technological chain. A classification of currently known and applied manufacturing technologies can be structured as follows:

a) Subtractive manufacturing technologies (material removal);
b) Formative manufacturing technologies (material redistribution), supporting industrial sustainability;
c) Rapid Prototyping (RP) and Additive Manufacturing (AM) technologies – this category is fundamentally different from the first two, as it is based on a different principle: the part is obtained by adding material exactly where and in the amount needed. These technologies directly produce a physical product, a prototype, or even a final part, starting from a 3D

digital model. This approach opens new perspectives in engineering, as it enables product customization, the fabrication of complex geometries impossible to achieve through conventional methods, and a reduction in time-to-market.

In conclusion, the shift from traditional processing technologies to modern, additive manufacturing–based approaches reflects a paradigm change in industrial production. Companies that successfully integrate these technologies into their manufacturing workflows benefit from greater flexibility, optimized costs, and enhanced capacity for innovation—key elements for long-term competitiveness.

Commonly referred to as AM, the basic principle of this technology is that a model, initially generated using a three-dimensional computer-aided design (3D CAD) system, can be manufactured without the need for extensive process planning. Although in practice this is not as simple as it sounds, AM certainly streamlines the production of complex objects directly from CAD data. Other manufacturing processes require a detailed analysis of the part geometry to determine aspects such as the order in which features can be produced, what tools and processes must be used, and what auxiliary devices may be necessary to complete the part. By contrast, AM requires only basic dimensional data and an understanding of how the AM machine and the chosen materials function.

1.2. The Main Stages in the Additive Manufacturing Process

All AM technologies involve a series of steps for transitioning from the CAD model to the physical result. Different products will employ AM in different ways and to varying degrees. Small, relatively simple products may use AM only for visualization models, while larger and more complex products may involve AM in multiple stages and iterations throughout the entire development process. Moreover, in the early stages of product development, unfinished parts may be sufficient, with AM being used primarily for the speed with which they can be produced. In later stages, however, the parts may require careful post-processing (including sanding, surface preparation, and painting) before they can be used, with AM proving useful due to the complexity of shapes that can be created.

Most AM processes involve, to some extent, the following eight steps:

- Step 1: Obtaining the CAD model
- Step 2: Conversion to STL format
- Step 3: Transferring the file to the AM machine
- Step 4: Machine setup
- Step 5: Building the part
- Step 6: Removing the part
- Step 7: Post-processing
- Step 8: Application/Use

Fields of application

Additive Manufacturing (AM) technologies are gaining an increasing number of application domains as processes mature and the range of compatible materials expands. While initially AM was used almost exclusively for the creation of visual or functional prototypes, its scope has now broadened considerably, encompassing not only the production of unique parts but also the manufacturing of small or even medium series of functional components.

One of the key reference tools for analyzing the evolution and adoption of these technologies is the Wohlers Report, which provides an annual global assessment of the AM market and its applications. According to the 2018 Wohlers Report, the distribution of AM application areas is presented in Figure 1.4, with the data highlighting a clear trend toward diversification and the consolidation of the role of these technologies in industry.

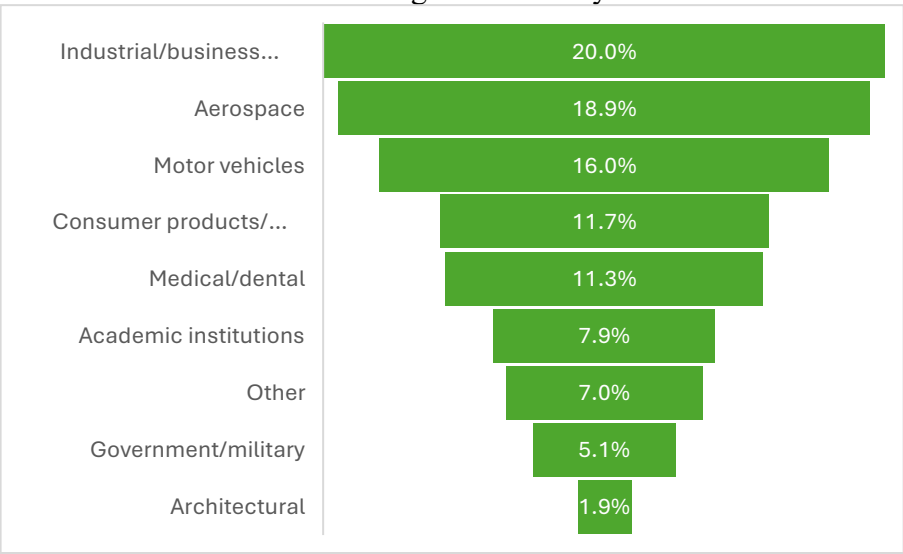


Fig. 1.4. AM fields of application

1.3. Advantages and disadvantages

1.3.1. Advantages

Geometric Complexity

One of the most evident and important advantages of additive manufacturing technologies is the almost unlimited freedom in creating complex shapes and geometries. In traditional subtractive manufacturing, constraints are always imposed by the technology used—whether casting, forging, or machining. These methods involve physical tools and instruments that limit dimensions, access angles, or the feasibility of producing intricate internal cavities. Consequently, the designer's creativity is inevitably restricted by technological and cost-related factors.

Reduction of the Number of Parts in a Subassembly

Another major advantage of additive manufacturing lies in the possibility of integrating into a single part functionalities that, in traditional manufacturing, would require the production and assembly of multiple distinct components. Since the additive process is not constrained by geometric limitations, the designer has the freedom to conceive complex structures with internal channels, joints, or regions of varying stiffness that can simultaneously fulfill the roles of several conventional parts.

Weight Reduction of Parts and Subassemblies

Additive manufacturing enables the design of components with complex internal structures such as voids, honeycomb patterns, or lattice frameworks—configurations impossible to achieve with conventional methods. These significantly reduce the mass of the components without compromising their strength. Moreover, by combining the functionality of multiple parts into a single component, the overall weight of subassemblies is reduced even further.

Reduced Costs

In most cases, additive technologies also reduce costs and expenditures in several ways. First, machine energy costs are generally low, particularly when considering the rapid turnaround of production. 3D printing technology also helps lower material and labor costs. Most importantly, it mitigates risks within the production workflow. By using additive technologies for rapid prototyping, companies can identify and correct design flaws before moving to final production, greatly reducing the risk of unnecessary expenses during manufacturing.

Customization

One of the key strengths of these technologies is the ability to achieve mass customization. Since 3D-printed components are generally produced one by one, designers and companies can modify or customize products as needed. *For example, in the field of medical prosthetics.*

Complete In-House Production of Parts

Another advantage of additive manufacturing is the possibility of producing parts entirely within the manufacturing company itself. Unlike subtractive production, where numerous stages of the manufacturing cycle are outsourced—such as casting, heat treatments, or special machining—in AM the entire part can be manufactured locally using only the 3D printing equipment and the base material.

1.4.2. Disadvantages

Limited Materials

One of the reasons why additive technologies are not always suitable for final production lies in the limitations regarding material selection. Since these objects are built layer by layer, the

resulting parts are generally weaker and less dense compared to CNC machining or injection molding. Nevertheless, the industry continues to advance in developing new materials.

Limited Dimensions

Build size is constrained by the printer's build volume, which means that printing cannot exceed the machine's predefined limits.

Accuracy

When producing parts that require high precision, additive technologies must be used with caution. Many materials are typically printed with an error margin of ±0.1 mm in accuracy. The 3D printing industry is continuously progressing in this respect, but it remains necessary to verify the accuracy of a machine before investing in an industrial 3D printer or service.

Production Limitations

Although 3D printing has undeniable value in rapid prototyping applications, there are significant limitations when it comes to production beyond that scope. While additive technologies can help save costs for prototypes and short-term production runs, these advantages often turn into disadvantages in mass production. Techniques such as injection molding and thermoforming still provide faster and more cost-effective solutions for final products, meaning that 3D printing has not yet reached this level of potential.

1.4. Clasification

There are numerous ways to classify AM technologies. One common approach is classification according to the type of process.

Photopolymerization occurs when a liquid photopolymer resin is exposed to light of a specific wavelength and undergoes a chemical reaction to become solid. Several additive technologies use this phenomenon to build a solid product layer by layer. The main technologies in this category include stereolithography (SLA), which uses either lasers or DLP (Digital Light Processing), and CLIP (Continuous Liquid Interface Production).

Stereolithography (SLA) is a process in which an object is created by selectively curing a polymer resin layer by layer using an ultraviolet (UV) laser beam. The materials used in SLA are photosensitive thermoset polymers in liquid form. SLA is recognized as the first 3D printing technology, patented in 1986. When highly accurate parts or fine surface finishes are required, SLA is the most cost-effective 3D printing technology available. Optimal results are obtained when designers take advantage of both the benefits and limitations of this process. SLA uses a build platform immersed in a transparent vat filled with liquid photopolymer resin. Once the platform is submerged, a single-point laser beam inside the machine traces the cross-sectional area (layer) of the part through the bottom of the vat, solidifying the material. After a layer is solidified, the platform rises, allowing fresh resin to flow beneath the part. This process repeats layer by layer until the final solid part is formed. Parts are typically post-cured with UV light to

improve their mechanical properties. SLA is a typical example of a layer-by-layer process based on the photopolymerization of a liquid.

Thermoplastic Extrusion (FDM – Fused Deposition Modelling) is one of the most widespread additive manufacturing technologies, belonging to the family of extrusion-based processes. Its principle involves the use of a thermoplastic polymer filament, heated to a temperature just below its melting point and extruded through a nozzle with a very small diameter, typically between 0.12 and 0.15 mm. The molten material is deposited onto a build platform, with the nozzle guided by a numerically controlled positioning system moving in the XOY plane to create the contour and fill of the current layer. By repeating this operation layer by layer, the three-dimensional object is built according to the CAD digital model.

Material Jetting (MJ) is an advanced additive manufacturing method based on the controlled jetting of liquid material followed by its layer-by-layer solidification. Conceptually, the process is similar to a two-dimensional inkjet printer; however, instead of ink, it uses liquid polymeric or composite materials that are cured by ultraviolet (UV) radiation. In this way, the three-dimensional model is created through successive deposition of thin layers, each immediately solidified to ensure adhesion to the previous one. The process starts with the distribution of material via high-precision nozzles moving horizontally across the build platform, depositing microscopic droplets of material according to the current layer's geometry. The droplets are then exposed to UV radiation, triggering instantaneous polymerization and transforming the liquid into solid material. This rapid solidification mechanism allows for smooth surfaces and fine details, often surpassing the resolution of other additive manufacturing technologies.

Nano Particle Jetting (NPJ) uses a liquid containing metallic nanoparticles or support nanoparticles, loaded into the printer as a cartridge and deposited onto the build tray in extremely thin layers of droplets. The high temperatures inside the build chamber cause the liquid to evaporate, leaving behind metallic parts.

Drop-On-Demand (DOD) Material Jetting Printers use two printheads: one to deposit the build material (often a wax-like liquid) and the other to deposit soluble support material. Similar to traditional AM techniques, DOD printers follow a predetermined path and deposit material point by point to build the cross-sectional area of a component. These machines also employ a wiper blade to spread material across the build area after each layer, ensuring a perfectly flat surface before printing the next layer.

Powder Bed Fusion Processes include commonly used techniques such as Direct Metal Laser Sintering (DMLS), Electron Beam Melting (EBM), Selective Laser Melting (SLM), and Selective Laser Sintering (SLS). These methods employ either a laser beam or an electron beam to melt and fuse powdered material together. The EBM process requires a vacuum but can be used with metals and alloys to create functional parts. All powder bed fusion processes involve spreading a thin layer of powder over the previous layer, using mechanisms such as a roller or a blade.

Laminated Object Manufacturing (LOM) is based on a layered construction process, in which each layer of the part is created by the successive deposition of thin sheets of material such

as specially treated paper, aluminum, or composites. These sheets are stacked and bonded together using a thermally activated adhesive layer, which is activated by a heated roller. After bonding, the outer contour and any internal cavities corresponding to each layer are cut with a laser beam or, in some cases, with a numerically controlled mechanical cutting system.

The manufacturing process begins with the transformation of the 3D model into a sequence of 2D cross-sections obtained through slicing along the Z-axis. These sections serve as reference planes for cutting each layer, and their successive stacking and bonding reconstruct the three-dimensional object. A distinctive feature of LOM technology, compared to other additive methods, is that in each step the entire material sheet is deposited, not just the part's contour area. The excess material outside the contour is not removed immediately but kept until the process is completed, where it serves as support for the upper layers.

Chapter 2. Tribostatics

Contact electrification, or static electricity, is the process by which electric charges are generated on the surface of different materials when they come into contact and are subsequently separated [1–6]. Tribo-charging, a specific type of contact electrification, occurs through frictional interactions and plays a significant role in numerous technological and industrial processes. Unlike simple contact electrification, which arises solely from contact and separation, tribo-charging involves mechanical friction, leading to a higher accumulation of charge due to repeated contact and the input of mechanical energy. The magnitude of tribo-charging depends on many factors, such as humidity, ambient temperature, impact velocity, flux density, and material composition [7–11].

2.1. Current state of research

Charging through the triboelectric effect is a complex surface phenomenon that is not yet fully understood. Researchers studying this effect have sometimes obtained contradictory results. Nevertheless, it is undeniable that the triboelectric effect depends on numerous factors: the nature of friction, the temperature of the contacting bodies, the surface condition of the samples, and ambient humidity appear to have the greatest influence on the generated charge.

Tribology is studied under three main aspects: friction (i.e., resistance to applied motion), wear (the loss of material), and lubrication (the interposition of a fluid between two bodies in contact).

The use of polymers in sliding contacts must take into account the triboelectric effect. Due to friction with another material, the polymer surface generates static charges that can accumulate during continuous friction cycles until reaching a certain saturation level, without being easily discharged to ground as in the case of metals. The uneven distribution of this charge

depends on the type of friction and can extend beyond the contact zone. This, to some extent, affects the wear behavior of polymers subjected to dry friction. Continuous contact between polymers generates electrical charges at their surfaces; combined with their low conductivity, this prevents efficient heat dissipation and leads to an increase in polymer temperature. The local interfacial temperature can become significantly higher than the ambient one and may be further amplified at asperity contacts by transient “flashes” or “hot spots.” Consequently, temperature has a direct influence on the wear of polymers [50].

Polymer tribology is the study of interactions between sliding surfaces, usually in the presence of a lubricant. It has been intensively studied since the mid-20th century and remains a subject of ongoing interest. It is important to recognize the multidisciplinary nature of tribology, which encompasses knowledge from materials science, surface chemistry and physics, solid and surface mechanics, thermal science, thermodynamics, and thermochemistry.

2.2. Triboelectric charging

Triboelectric charging, or charging by friction, is the phenomenon that describes the transfer of electric charge between two electrically neutral objects that are either rubbed against each other or simply brought into contact . As a result of this process, the two bodies acquire electric charges of opposite polarity. The generated charge persists after separation, and each new contact produces a new charge transfer.

Triboelectric charge is difficult to predict due to the complexity of the influencing factors, such as the nature of the materials, their roughness, relative pressure and velocity, as well as the temperature and humidity of the surrounding environment.

The first scientific reference to the phenomenon of triboelectrification is attributed to Thales of Miletus (640–546 BC), who rubbed amber with various materials such as silk, cat fur, or wool, then used the electrostatically charged amber to attract other lightweight materials such as threads, straw, hay, dried leaves, feathers, and down.

The triboelectric effect can be explained by several physical mechanisms arising from the transfer of electrons, ions, or matter at the contact interface. In general, the amount of transferred charge increases with:

- contact roughness,
- contact area,
- contact velocity.

Chapter 3. Conclusions on the state of the art

Additive manufacturing (AM) technologies have rapidly evolved from prototyping to complex industrial solutions with applications across diverse fields. However, they still present significant limitations, such as high costs, low production speed, restricted build volume, limited material diversity, and surface quality issues.

Surface quality is a critical factor, influencing not only appearance and dimensional accuracy but also functional properties such as mechanical strength and electrostatic performance. For this reason, methods to optimize surface texture directly during the AM process are being sought, in order to reduce dependence on post-processing.

In parallel, triboelectricity has become a field of great interest, particularly with the development of triboelectric nanogenerators (TENGs), capable of converting ambient mechanical energy into usable electrical energy. Their performance depends on the materials employed and the topography of the contact surfaces. Roughness and surface geometry directly affect the generated charge and its stability.

The convergence of AM and triboelectricity opens new research directions: producing controlled surface textures via 3D printing allows optimization of the tribo-charging process while offering precision, flexibility, and reproducibility.

The field remains insufficiently explored, requiring comparative studies, predictive models linking printing parameters to triboelectric performance, long-term stability analyses, and the exploration of sustainable polymeric materials.

The intersection between AM and triboelectricity thus represents an emerging research direction, with high potential both for advancing fundamental understanding and for developing innovative applications in energy and self-powered devices.

Part II. Contributions to the study of the triboelectric behaviour of polymer 3d printed surfaces

Chapter 4. Directions, main objective and research-development methodology

4.1. Research directions

Based on the findings from the analysis of the current state of research, the following research and development directions are considered timely regarding additive manufacturing and its influence on triboelectrostatic phenomena:

- optimization of 3D printing process parameters to obtain polymer surfaces with controlled and reproducible textures;
- investigation of the relationship between surface morphology (roughness, texture geometry, build orientation) and the level of generated tribo-charging;
- analysis of the long-term stability of the electrostatic potential accumulated on AM-produced surfaces, depending on the type of texturing and the material used;
- comparison of the triboelectric performance of different types of polymers, with emphasis on biodegradable and sustainable materials (e.g., PLA);
- development of conceptual and experimental models enabling correlations between AM parameters and triboelectric performance, with a view toward energy applications (e.g., triboelectric nanogenerators – TENGs).

4.2. Main objective

Considering the data and conclusions drawn from the analysis of the current state of the art, as well as the identified research and development directions, the main objective of this doctoral research is defined as follows:

The study of the triboelectric behavior of polymer surfaces obtained by additive manufacturing and the identification of the relationship between 3D printing parameters, surface texture, and the level of tribo-charging, with the aim of optimizing these factors for energy applications.

4.3. Research and development methodology

The research and development methodology is conceived as a reference framework for the actions to be undertaken in order to achieve the main objective of the doctoral work, as well as for future development directions.

The methodological reference elements are as follows:

1. Analysis of the scientific literature – to identify the current state of knowledge regarding AM technologies, surface quality, and their influence on triboelectrostatic phenomena.
2. Design and fabrication of experimental samples – by FDM-type 3D printing, using varied process parameters (orientation, layer thickness, infill pattern, types of texturing).
3. Characterization of the obtained surfaces – using specific methods (optical and electron microscopy, roughness determination, dimensional analysis) to evaluate surface morphology and integrity.
4. Determination of electrostatic potential – employing dedicated measuring equipment (e.g., electrostatic voltmeter, universal tribometer) under controlled contact and separation conditions.
5. Comparative analysis of results – to establish correlations between printing parameters, surface texture, and the obtained triboelectric performance.
6. Formulation of conclusions and recommendations – regarding the optimization of additively manufactured surfaces for improved level and stability of triboelectric charging, with applicability in the energy field and self-powered devices.

4.4. Materials and methods

A. Sample design and manufacturing

In recent years, additive manufacturing technologies have been increasingly applied in academic and industrial fields to improve material performance and enhance energy efficiency, being regarded as next-generation solutions with advantages such as cost reduction, production speed, accessibility, sustainability, and the ability to create complex geometries [51]. Fused Deposition Modelling (FDM) is one of the most widely used 3D printing technologies. It is known for the variety of materials available, the ease of material change, low maintenance costs, and the capability to rapidly produce thin parts with a general tolerance of ±0.1 mm, without supervision, in compact sizes, and at relatively low operating temperatures.

Polylactic acid (PLA) is a low-cost and sustainable 3D printing material, as it is bio-based and biodegradable [52]. The choice of PLA for experiments is further justified by the fact that it is the most commonly used thermoplastic in FDM printing. Although it has lower plasticity compared to acrylonitrile butadiene styrene (ABS), it exhibits higher mechanical strength. For the 3D printing of the samples, a red PLA filament with a diameter of 1.75 mm, brand RS PRO, was selected. The 3D models of the samples were created in SolidWorks software and exported in STL (Standard Tessellation Language) format. Geometric codes were generated using the slicing software IdeaMaker.

Three types of samples were prepared using the FDM technique. All samples were fabricated with a durable, fully enclosed 3D printer, model RAISE3D E2 (Raise 3D Technologies Inc.). The main feature of the E2 printer is its independent dual-extruder technology, with mirror and duplication modes, which proved very useful for improving time efficiency in the study.

The main technological parameters selected for sample printing are presented in Table 2. The three types of samples, referred to in this study as “lines,” “zigzag,” and “waves” (Figure 8), were fabricated with dimensions of 50 mm × 50 mm × 5 mm and a texture depth of 1 mm. The CAD versions and the physical prints showed significant variations, attributed to the susceptibility of PLA to shrinkage, with a dimensional error of up to ±0.5 mm.

Table 2. Main technological parameters selected for sample printing

	Parameter	Value
Process-based parameters	Melting temperature	200 °C
	Bed temperature	50 °C
	Printing speed	70 mm/s
Structural parameters	Layer thickness	0.1 mm
	Infill geometry	Gyroid
	Infill density	10%

B. Triboelectric test bench

The experiments were carried out using a **linear tribometer** (Fig. 9) to generate electric charge through the friction of two samples (A and B – Fig. 10).

One method of determining which materials work best together to generate static charges through friction is by consulting the **triboelectric series**. When rubbed together, materials positioned higher in the list acquire a positive charge (electron loss), while those positioned lower acquire a negative charge (electron gain). The further apart the two materials are in this series, the stronger the generated charge.

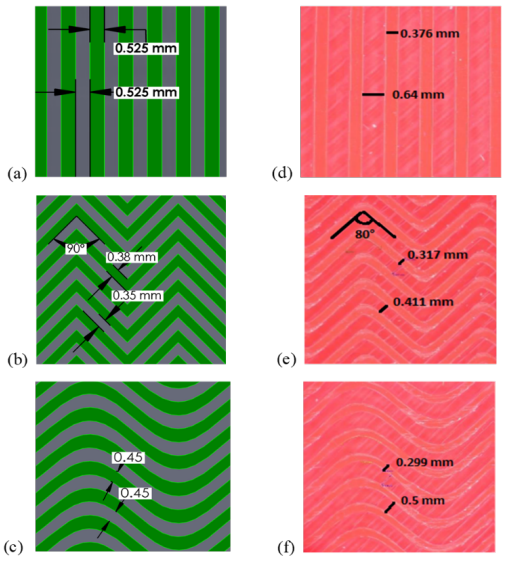


Fig. 8. CAD models of the textured PLA samples: (a) "lines," (b) "zigzag," (c) "waves," and microscopic images (Makrolite 4K, Vision Engineering Ltd) of the printed samples: (d) "lines," (e) "zigzag," (f) "waves."

As shown in Fig. 9, the PLA sample B is attached to a linear motion system (1), which moves back and forth, driven by a linear electric motor (4).

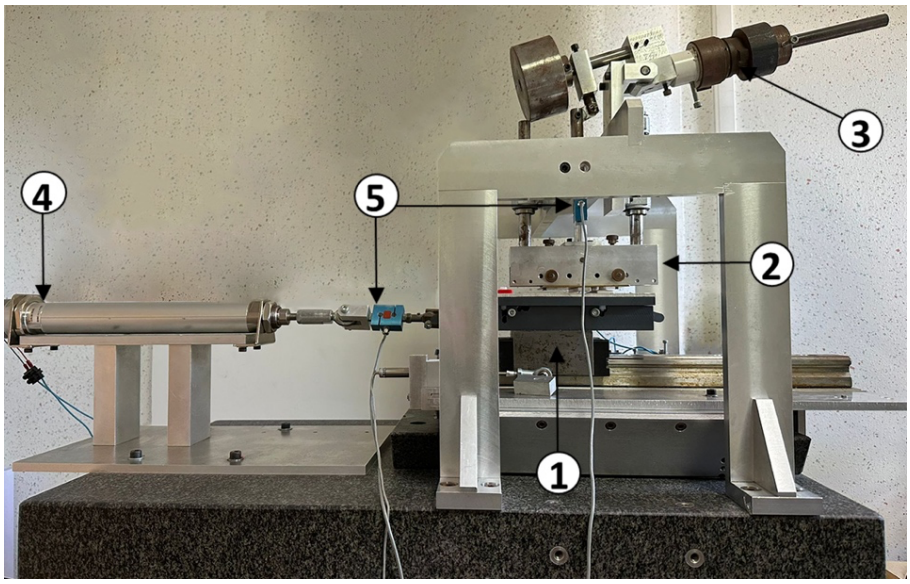


Fig. 9. Laboratory test stand for the triboelectric charging of polymer plates: 1 – sliding motion system driving sample B in a back-and-forth movement; 2 – upper holder with attached sample A; 3 – lever-type device for adjusting the normal contact force; 4 – linear motor; 5 – force sensors.

Sample A is connected to an upper holder (2), fixed in a vertical guiding system, while the normal force is manually controlled by a lever-type mechanism (3). The tangential and normal forces, as well as the relative displacements of the samples, are continuously measured using the sensors (5).

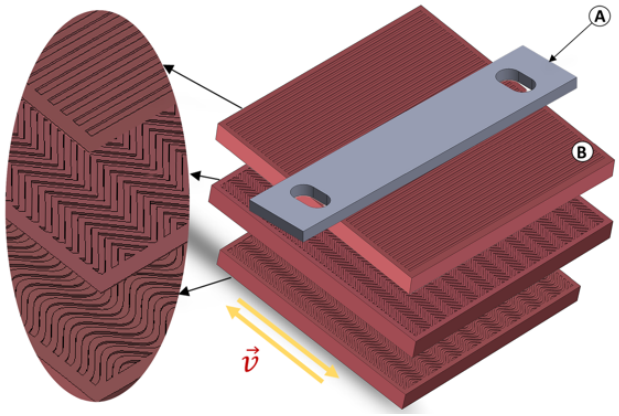


Fig. 10. Relative frictional motion between samples A (Aluminum) and B (PLA).

The test bench setup enables precise control of the factors influencing the tribo-charging process, including relative sliding speed, stroke length, and the number of friction cycles. These parameters are programmed and controlled through the LabVIEW software, ensuring consistency throughout the experiments.

C. Electrostatic probe

In the experiments, the distribution of electric charge on the sample surfaces was evaluated using an induction probe (Trek, model 6300-7) connected to a high-sensitivity electrostatic voltmeter (Trek, model 341B). This experimental setup was mounted on a two-axis device, enabling precise mapping of the surface potential across the entire sample area (Fig. 11). The system ensured controlled displacement of the probe above the sample, maintaining a constant distance and guaranteeing measurement repeatability.

To achieve a detailed characterization, measurements were performed along 14 parallel lines, spaced at 2 mm, covering the surface from the near-left corner to the far-right corner of the sample. This sampling strategy allowed the identification of local potential variations and possible non-uniformities generated by the friction process or by specific features of the surface structure.

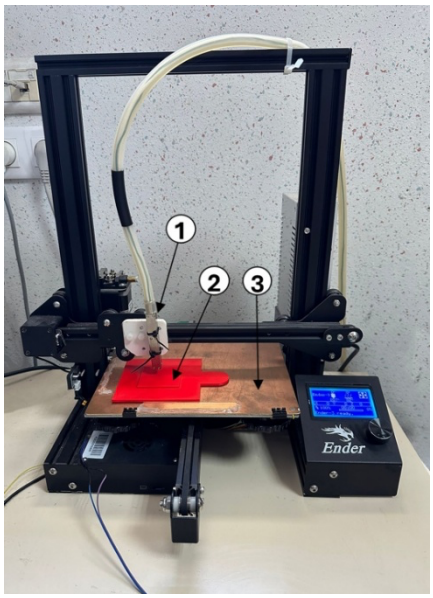


Fig. 11. Two-axis device for surface potential mapping: 1 – electrostatic probe; 2 – sample B; 3 – grounded plate.

D. Tribological measurments

During the experiments, the upper specimen (the pin) was progressively lowered until it touched the surface of the PLA sample, thus establishing the initial contact. The applied normal force was 20 N, a value chosen to reproduce as accurately as possible the conditions of previous tests performed on the linear tribometer and to allow a direct comparison of the results. Once contact was established, the pin slid over the flat surface of the sample, generating a stable and reproducible frictional contact.

Throughout the measurements, the applied normal force remained practically constant, due to the high stiffness of the tribometer's force sensor. This stability allowed for the acquisition of precise and reproducible data regarding the tribological behavior of the samples. During the tests, a normal load F was applied, while in parallel the friction force Ff was recorded as the aluminum pin slid over the PLA sample surface at a preset sliding speed. This method enabled the determination of the evolution of the coefficient of friction over time and the analysis of the relationship between the mechanical contact conditions and the triboelectric charging phenomena observed at the polymer surface. The results obtained provide a solid basis for correlating the tribological behavior of polymeric materials with their electrostatic properties.

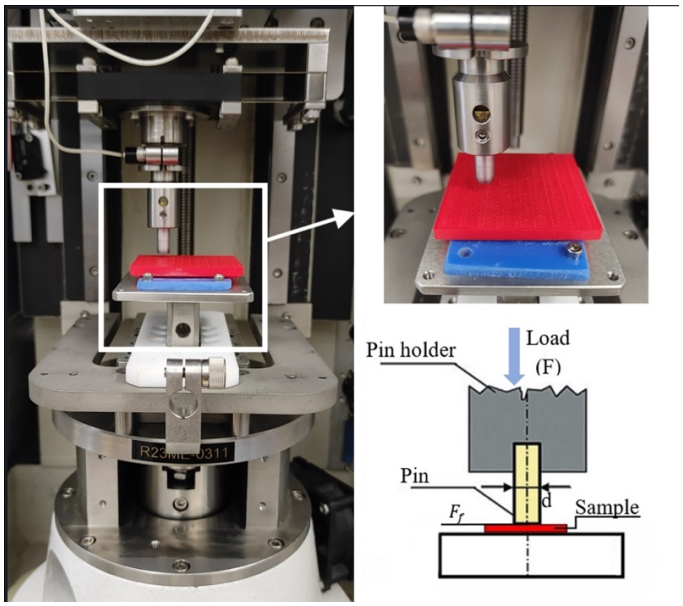


Fig. 12. Tribometer configuration (UMT-2 (CETR)) and schematic representation

Subsequently, for the detailed characterization of the surface, the MarSurf GD 140 instrument (Mahr GmbH, Germany) was used (Fig. 13). This equipment is a state-of-the-art

precision instrument, designed for the evaluation of surface roughness and waviness with a high degree of accuracy. In the context of additive manufacturing, where layer-by-layer quality directly influences both the mechanical properties and the triboelectric behavior of the parts, detailed analysis of surface texture becomes essential.

The MarSurf GD 140 measurement station combines a robust mechanical design with sophisticated software that facilitates data acquisition and interpretation. The measuring sensor moves precisely across the surface of the sample, recording microscopic deviations from the ideal profile. The collected data are then processed by the dedicated software, which enables graphical visualization and calculation of specific roughness and waviness parameters.

The instrument's capabilities include measuring standardized topography parameters in accordance with ISO 25178-2:2021, ensuring the comparability of the obtained results with data reported in the international literature. The extracted parameters provide comprehensive information about surface characteristics such as roughness amplitude, irregularity distribution, or degree of uniformity. This information is indispensable for evaluating part quality, optimizing printing parameters, and correlating topography with the triboelectric phenomena under study.

Therefore, the use of the MarSurf GD 140 provided a detailed picture of the topography of 3D-printed surfaces, constituting a solid basis for analyzing the relationship between roughness and the electrostatic charging induced during tribological tests.

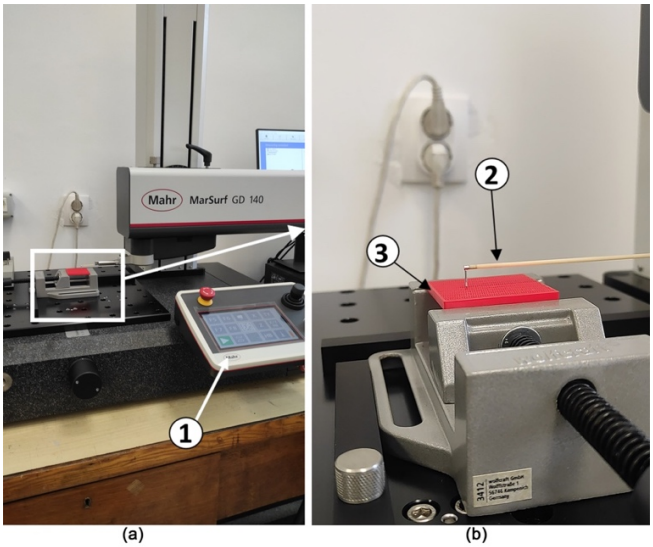


Fig. 13. MarSurf GD 140 Tribometer (Mahr GmbH): a) General view of the configuration: 1 – control panel, 2 – measuring probe, 3 – sample; b) Detailed view of the measuring probe arm.

E. Experimental procedure

Based on the results of previous studies [35],[36], the test bench parameters were chosen as follows:

- Normal force: 20 N
- Translation speed: 20 mm/s
- Stroke of the lower sample holder: 50 mm
- Number of friction cycles: 20 and 40, respectively

To avoid the results being influenced by possible surface damage caused by the aluminum sample, material transfer, or residual loads, a new sample was used for each experiment, thus ensuring reproducibility.

The first series of experiments consisted of charging the surface of the PLA samples using the tribocharging stand for 20 and 40 cycles with an aluminum bar. The triboelectrically charged samples were then scanned with the electrostatic voltmeter, driven by the 2D mapping system, to map the distribution, variations, and patterns of the electric potential — reflecting the distribution of the electric charge.

The second series of experiments consisted of charging the PLA samples with the tribocharging stand for 20 and 40 cycles, after which they were placed under the probe of the electrostatic voltmeter for 10 minutes each, in order to measure the evolution of the surface potential — reflecting the surface potential decay (SPD) curve — over time, in a fixed area, specifically at the center of the sample. This approach enabled monitoring of how the surface charge dissipates at a single constant location throughout the experiments. The 10-minute endpoint for the second series of experiments was chosen because, by that time, the electric potential had decayed to less than one quarter of its initial value, and further measurements would not have provided significant additional information about the decay process.

4.5. Results

Table 3 presents the values of the electric potential dispersion for the three types of textures analyzed. Among them, the lowest dispersion, of approximately 15%, was recorded for the PLA sample surface with the “lines” texture. This reduced value suggests a more uniform behavior and superior stability of the accumulated electric charge, which can be attributed to the simple and repeatable geometries of this texture.

In comparison, more complex textures such as “zigzag” and “waves” generated higher dispersions, reflecting a less uniform distribution of the electric charge on the surface. These differences indicate that topography plays a decisive role in the way triboelectric charge is accumulated and dissipated. Thus, the “lines” texture proves to be the most predictable and stable among the analyzed variants, making it more suitable for applications that require consistency in electrostatic behavior.

Table 3. Comparison of the dispersion of potential values recorded for the three types of samples

Texture	Cycles	Min (V)	Max (V)	Average (V)	Range (V)	Disp/Aver
Lines	20 Cyc	163	191	179	28	15%
	40 Cyc	328	412	364	84	28%
Zigzag	20 Cyc	183	277	227	94	41%
	40 Cyc	451	830	524	379	72%
Waves	20 Cyc	709	1010	859	301	35%
	40 Cyc	555	1595	1123	1040	92%

D. Coefficient of friction and friction force

The dry friction tests with reciprocating motion were carried out on the UMT-2 (CETR) tribometer, under ambient temperature conditions and relative humidity of 50–60%. The testing parameters were: 1 stroke, duration of 30 seconds, sliding distance of 30 mm, and normal force of 20 N. Figures 23 and 24 show how the friction force and the coefficient of friction vary for all analyzed surfaces as a function of elapsed time. The values were recorded at a frequency of 100 Hz.

The coefficient of friction (CoF) is calculated as the ratio between the friction force (Ff) and the corresponding normal force. In the context of the two-stage friction behavior observed in all three types of samples, the initial rapid increase of the CoF in the first stage (first 5 seconds) can be explained by the transition from static friction to kinetic friction. Initially, the friction force is generated mainly by static friction, which resists the initiation of motion. Once motion begins, the friction force becomes kinetic, leading to the observed peak in the CoF.

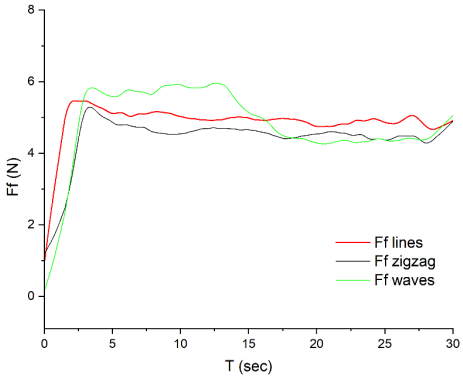


Fig. 23. Variation of friction force as a function of time.

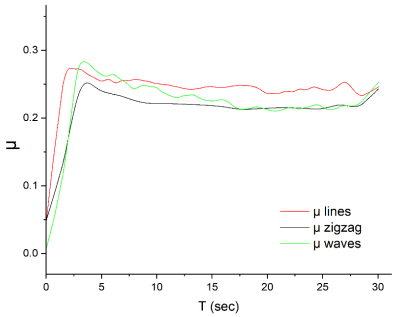


Fig. 24. Variation of the coefficient of friction as a function of time

In the second stage, as sliding continues, the friction force stabilizes, and the CoF becomes constant. This occurs because the kinetic friction force remains steady after the initial adjustment phase, once the surfaces of the two bodies are already in relative motion. The fluctuations of the CoF in this stage can be attributed to variations in the surface profile over which the pin slides. In this phase, the friction force is influenced mainly by the nature of the contact surfaces and the normal force.

The shorter duration of the first stage in the case of the "lines" texture suggests that this surface has a lower static friction force, allowing a faster transition to kinetic friction. After this transition, the coefficient of friction stabilizes, reflecting the predominance of kinetic friction. Figure 25 illustrates the maximum and average coefficients of friction, as well as the friction force, for all samples. Despite differences in magnitude, the variation of the coefficient of friction is very similar in all cases. The relatively high friction values in all three cases support the presence of electric charge on the sample surfaces. Moreover, the surface with the highest CoF was the one with the "waves" texture, which also exhibited the highest charge, confirming the link between roughness and the level of charging.

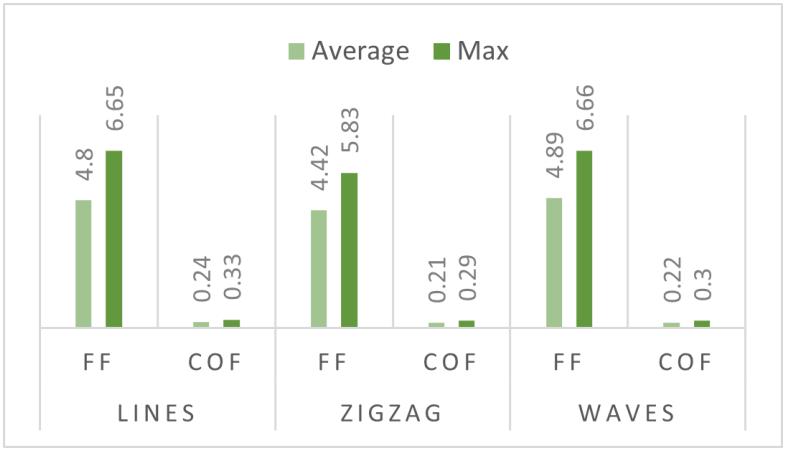


Fig. 25. Comparative graph of maximum and average friction coefficient and friction force values for the three sample types

E. Roughness parameters

The purpose of the measurements was to compare the roughness parameters Ra/Sa and Rz/Sz for the three types of samples, as indicators of surface quality. The results showed that the "waves" texture exhibited the highest values for all analyzed parameters, confirming the hypothesis that increased roughness favors charge accumulation by enlarging the contact areas and intensifying the local electric field. Therefore, the relationship between roughness and triboelectric potential is direct, with rougher surfaces accumulating higher levels of charge. This conclusion plays an essential role in optimizing the texture of 3D-printed polymeric surfaces for specific applications.

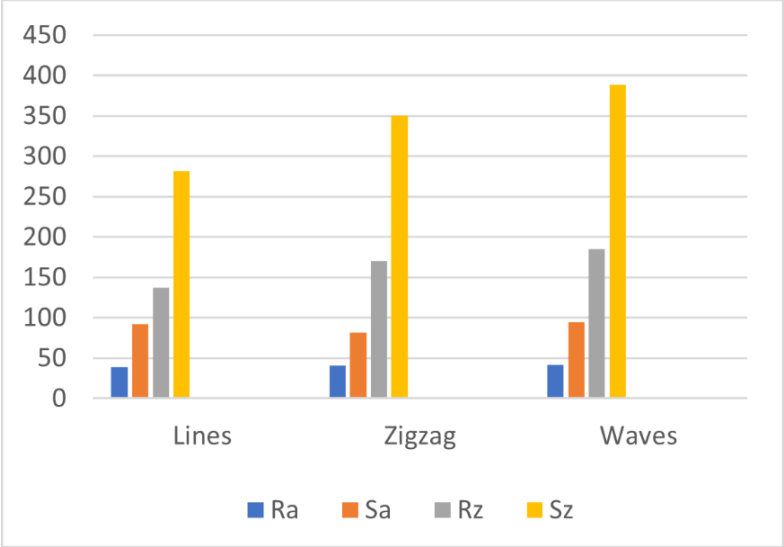


Fig. 29. Average Ra/Sa (µm) and Rz/Sz (µm) values for the three different texture types

4. Conclusions

The objective of this work was to investigate the influence of three types of 3D-printed PLA textures on the triboelectric charging that occurs upon contact with aluminum. The measurements showed that the "lines" and "zigzag" textures generate similar levels and dispersions of potential, while the "waves" texture produces values more than twice as high, maintained even after 20 and 40 friction cycles. The decay curves confirm this distinct behavior, with the initial potential of the "waves" texture being clearly superior to the others. At the same time, the tribological tests revealed higher values of the coefficient of friction and wear for the same texture. The results can be correlated with the surface roughness and highlight the need for further studies on different materials and morphologies, in order to support the application of 3D-printed polymers in energy harvesting, medical devices, and small-scale electronics.

Chapter 5. Final conclusions and main contributions

5.1. Final conclusions

From the analysis of the current state of the art, it results that additive manufacturing technologies offer significant advantages (complex geometries, material reduction, flexibility), but also limitations (costs, limited range of materials, surface quality). In the field of triboelectricity, surface morphology is essential for charge generation and stability; however, its correlation with 3D printing parameters is still little studied. Thus, the main objective of this thesis was to investigate the triboelectric behavior of 3D-printed polymer surfaces and to establish the relationships between process parameters, surface texture, and charging level, with the aim of optimizing them for energy applications.

The results showed that the type of texturing, roughness, printing orientation, and layer thickness directly influence the level and stability of the charge: linear textures provide uniform distributions, sinusoidal ones yield maximum but variable values, and increased roughness generates high initial charges with rapid dissipation. The developed testing methodology proved to be reproducible and applicable to future optimization research.

5.2. Main contributions

The thesis brings original contributions by developing an integrated experimental methodology for characterizing the triboelectric behavior of 3D-printed polymer samples, with clear procedures for preparation and reproducible measurement. Textured surfaces with varied geometries (lines, grids, sinusoidal shapes) were produced and tested, systematically explored for the first time in the specialized literature. Direct correlations between printing parameters (orientation, layer thickness) and the level or stability of the accumulated electric charge were also identified. Another contribution consists in establishing the use of biodegradable materials (PLA) in triboelectric applications, highlighting both their sustainability and functional potential. In addition, application-oriented directions were proposed for integrating 3D-printed surfaces into triboelectric nanogenerators and complementary energy systems, demonstrating the transfer of research toward practical applications in renewable energy and smart technologies.

5.3. Importance of the thesis

This thesis makes a relevant contribution to the development of the interdisciplinary field between additive manufacturing and triboelectric phenomena, exploring an insufficiently studied area with significant scientific and technological potential in the context of green energy and novel materials. The original contributions consist in demonstrating the link between the texture of 3D-printed surfaces and the level of triboelectric charging, providing a solid foundation for understanding fundamental mechanisms and for developing predictive models. The practical importance is reflected in the validation of a methodological framework applicable both in fundamental research and in industry, with useful results for optimizing AM processes and

designing surfaces for triboelectric nanogenerators. Furthermore, the proposed methodology supports academic training and specialists interested in emerging applications of Industry 4.0 and sustainable technologies.

5.4. Future perspectives

The issues addressed in this thesis require ongoing research, aimed at extending studies to a wider range of polymeric and composite materials, with emphasis on biodegradable and sustainable variants, relevant in the context of the ecological transition. Advanced characterization methods (AFM, FEM, local charge measurements) are essential for a detailed understanding of triboelectric mechanisms at the micro- and nanoscale, as well as the development of predictive numerical models that correlate 3D printing parameters with the resulting performance. In addition, integrating optimized surfaces into functional prototypes of triboelectric nanogenerators would validate the applicability of the results, opening perspectives for practical implementations in autonomous sensors, wearable devices, or energy recovery systems.

Bibliography

[1] A.F. Diaz, R.M. Felix-Navarro, A semi-quantitative tribo-electric series for polymeric materials: the influence of chemical structure and properties, J. Electrost. 62 (2004) 277–290. https://doi.org/10.1016/j.elstat.2004.05.005.

[2] G.W. Follows, J. Lowell, M.P.W. Wilson, Contact electrification of polyamides, J. Electrost. 26 (1991) 261–273. https://doi.org/10.1016/0304-3886(91)90021-7.

[3] J. Lowell, A.C. and Rose-Innes, Contact electrification, Adv. Phys. 29 (1980) 947–1023. https://doi.org/10.1080/00018738000101466.

[4] U.G. Musa, S.D. Cezan, B. Baytekin, H.T. Baytekin, The Charging Events in Contact-Separation Electrification, Sci. Rep. 8 (2018) 2472. https://doi.org/10.1038/s41598-018-20413-1.

[5] D.J. Lacks, R. Mohan Sankaran, Contact electrification of insulating materials, J. Phys. Appl. Phys. 44 (2011) 453001. https://doi.org/10.1088/0022-3727/44/45/453001.

[6] L.S. McCarty, G.M. Whitesides, Electrostatic Charging Due to Separation of Ions at Interfaces: Contact Electrification of Ionic Electrets, Angew. Chem. Int. Ed. 47 (2008) 2188–2207. https://doi.org/10.1002/anie.200701812.

[7] J.N. Rasera, R.D. Cruise, J.J. Cilliers, J.-A. Lamamy, K. Hadler, Modelling the tribocharging process in 2D and 3D, Powder Technol. 407 (2022) 117607. https://doi.org/10.1016/j.powtec.2022.117607.

[8] S. Trigwell, N. Grable, C.U. Yurteri, R. Sharma, M.K. Mazumder, Effects of surface properties on the tribocharging characteristics of polymer powder as applied to industrial processes, IEEE Trans. Ind. Appl. 39 (2003) 79–86. https://doi.org/10.1109/TIA.2002.807228.

[9] K. Saleh, A. Traore Ndama, P. Guigon, Relevant parameters involved in tribocharging of powders during dilute phase pneumatic transport, Chem. Eng. Res. Des. 89 (2011) 2582–2597. https://doi.org/10.1016/j.cherd.2011.06.001.

[10] O. Tilmatine, T. Zeghloul, K. Medles, L. Dascalescu, A. Fatu, Effect of ambient air relative humidity on the triboelectric properties of Polypropylene and Polyvinyl Chloride slabs, J. Electrost. 115 (2022) 103651. https://doi.org/10.1016/j.elstat.2021.103651.

[11] T.A.L. Burgo, C.A. Silva, L.B.S. Balestrin, F. Galembeck, Friction coefficient dependence on electrostatic tribocharging, Sci. Rep. 3 (2013) 2384. https://doi.org/10.1038/srep02384.

[12] E. Nikitina, H. Barthel, M. Heinemann, Electron Transfer in Electrical Tribocharging Using a Quantum Chemical Approach, J. Imaging Sci. Technol. 53 (2009) 040503. https://doi.org/10.2352/J.ImagingSci.Technol.2009.53.4.040503.

[13] D. Tan, M. Willatzen, Z.L. Wang, Electron transfer in the contact-electrification between corrugated 2D materials: A first-principles study, Nano Energy 79 (2021) 105386. https://doi.org/10.1016/j.nanoen.2020.105386.

[14] C. Xu, Y. Zi, A. Wang, H. Zou, Y.-J. Dai, X. He, P. Wang, Y.-C. Wang, P. Feng, D. Li, Z. Wang, On the Electron-Transfer Mechanism in the Contact-Electrification Effect, Adv. Mater. 30 (2018) 1706790. https://doi.org/10.1002/adma.201706790.

[15] M. Beckschulte, E. Taglauer, The influence of work function changes on the charge exchange in low-energy ion scattering, Nucl. Instrum. Methods Phys. Res. Sect. B Beam Interact. Mater. At. 78 (1993) 29–37. https://doi.org/10.1016/0168-583X(93)95772-W.

[16] A.F. Diaz, D. Fenzel-Alexander, An ion transfer model for contact charging, Langmuir 9 (1993) 1009–1015. https://doi.org/10.1021/la00028a021.

[17] R. Pandey, H. Kakehashi, H. Nakanishi, S. Soh, Correlating Material Transfer and Charge Transfer in Contact Electrification, J. Phys. Chem. C 122 (2018). https://doi.org/10.1021/acs.jpcc.8b04357.

[18] R. Holm, Theory of the electric material transfer in switching contacts. History of this theory, in: R. Holm (Ed.), Elektr. Kontakte Electr. Contacts Handb., Springer, Berlin, Heidelberg, 1958: pp. 376–387. https://doi.org/10.1007/978-3-662-25893-4_66.

[19] D.S. Rimai, D.S. Weiss, M. Cristina de Jesus, D.J. Quesnel, Electrophotography as a means of microfabrication: the role of electrodynamic and electrostatic forces, Comptes Rendus Chim. 9 (2006) 3–12. https://doi.org/10.1016/j.crci.2004.10.030.

[20] C.B. Duke, J. Noolandi, T. Thieret, The surface science of xerography, Surf. Sci. 500 (2002) 1005–1023. https://doi.org/10.1016/S0039-6028(01)01527-8.

[21] H. Moulai, T. Zeghloul, N. Menad, L. Dascalescu, Effect of high voltage and electrode configuration on the trajectories of metallic particles in roll-type electrostatic separators for granular mixtures, J. Electrost. 133 (2025) 104014. https://doi.org/10.1016/j.elstat.2024.104014.

[22] T. Zeghloul, A. Mekhalef Benhafssa, G. Richard, K. Medles, L. Dascalescu, Effect of particle size on the tribo-aero-electrostatic separation of plastics, J. Electrost. 88 (2017) 24–28. https://doi.org/10.1016/j.elstat.2016.12.003.

[23] G. Bedeković, R. Trbović, Electrostatic separation of aluminium from residue of electric cables recycling process, Waste Manag. 108 (2020) 21–27. https://doi.org/10.1016/j.wasman.2020.04.033.

[24] A. Reguig, A. Bendaoud, P. Dordizadeh, A.R. Salama, S. Messal, L. Dascalescu, Experimental study of a modified dual-type high-voltage electrode for electrostatic separation applications, J. Electrost. 88 (2017) 232–235. https://doi.org/10.1016/j.elstat.2016.12.007.

[25] L. Dascalescu, T. Zeghloul, K. Medles, A. Iuga, Recent advances in the electrostatic separation of particulate matter, J. Electrost. 134 (2025) 104036. https://doi.org/10.1016/j.elstat.2025.104036.

[26] Y. Tian, J. Yin, T. Ma, W. Yan, H. Zhu, H. Sun, Study on electrostatic separation technology and characterization of shrimp shell protein, Sep. Purif. Technol. 354 (2025) 128862. https://doi.org/10.1016/j.seppur.2024.128862.

[27] K. Daioui, T. Zeghloul, N. Perbet, L. Dascalescu, Tribo-electrostatic separation of plastic flakes originating from packaging waste, J. Electrost. 134 (2025) 104046. https://doi.org/10.1016/j.elstat.2025.104046.

[28] Q. Wang, T. Wang, Y. Liu, S. Xie, S. Du, Y. Li, J. Yu, L. Zhang, D. Li, D. Li, Y. Guo, X. Wang, 3D visualization microscope of TENG contact interface based on astigmatic imaging, Nano Energy 129 (2024) 110061. https://doi.org/10.1016/j.nanoen.2024.110061.

[29] A novel polymer composite from polyhexamethylene guanidine hydrochloride for high performance triboelectric nanogenerators (TENGs), RSC Adv. 15 (2025) 844–850. https://doi.org/10.1039/d4ra07768g.

[30] J. Ye, C. He, X. Gong, H. Zhang, X. Li, Blue energy harvesting based on triboelectric nanogenerators (TENG): Structural design, performance optimization, and application prospects, J. Alloys Compd. 1014 (2025) 178710. https://doi.org/10.1016/j.jallcom.2025.178710.

[31] F. Xing, G. Tang, H. Wang, M. Wang, M. Wu, M. Xu, Exploring the synergy of EMG and TENG in motion based hybrid energy harvesting, Nano Energy 134 (2025) 110584. https://doi.org/10.1016/j.nanoen.2024.110584.

[32] W. Wang, N. Yin, Z. Wu, Z. Zhang, Omnidirectional energy harvesting with 3D-TENG for vibration diagnosis, Chem. Eng. J. 509 (2025) 161022. https://doi.org/10.1016/j.cej.2025.161022.

[33] J. Wang, P. Li, X. Kang, Z. Li, S. Dai, Soft-soft contact TENG using nonlinear coupling galloping phenomenon for harvesting wind energy, Nano Energy 133 (2025) 110471. https://doi.org/10.1016/j.nanoen.2024.110471.

[34] S. Qiu, X. Teng, Y. Zhang, X. Wang, K. Chen, J. Zhao, Q. Huang, Wearing comfortable and high electrical output TENGs woven with PTFE core–shell nanofiber yarns, Chem. Eng. J. 505 (2025) 159501. https://doi.org/10.1016/j.cej.2025.159501.

[35] Electrostatic properties of powder coatings, Focus Powder Coat. 2010 (2010) 3–5. https://doi.org/10.1016/S1364-5439(10)70051-4.

[36] Y. Tabata, S. Masuda, Minimum Potential of Charged Insulator to Cause Incendiary Discharges, IEEE Trans. Ind. Appl. IA-20 (1984) 1206–1211. https://doi.org/10.1109/TIA.1984.4504584.

[37] M. Glor, Electrostatic ignition hazards in the process industry, J. Electrost. 63 (2005) 447–453. https://doi.org/10.1016/j.elstat.2005.03.001.

[38] W.D. Greason, Electrostatic discharge in electronics, Research Studies Press and J. Wiley, 1992. https://cir.nii.ac.jp/crid/1130282272766702336 (accessed March 28, 2025).

[39] J. Pionteck, G. Wypych, eds., 4 - ELECTROSTATIC HAZARDS, in: Handb. Antistatics Second Ed., ChemTec Publishing, 2016: pp. 65–73. https://doi.org/10.1016/B978-1-895198-95-9.50006-6.

[40] S. Cho, M.R. Khawar, Y. Ra, S. Jang, D. Lee, D. Kam, S.A. Shah, D. Yoo, Y. Javed, A. Ahmad, Y. Lee, H.J. Hwang, C. Lee, D. Choi, Advances in 3D-printed triboelectric nanogenerators and supercapacitors for self-sustainable energy systems, Mater. Today (2025). https://doi.org/10.1016/j.mattod.2025.02.010.

[41] S. Akin, T. Chang, S.S.H. Abir, Y.W. Kim, S. Xu, J. Lim, Y. Sim, J. Lee, J.-T. Tsai, C. Nath, H. Lee, W. Wu, J. Samuel, C.H. Lee, M.B.-G. Jun, One-step fabrication of functionalized electrodes on 3D-printed polymers for triboelectric nanogenerators, Nano Energy 129 (2024) 110082. https://doi.org/10.1016/j.nanoen.2024.110082.

[42] Influence of 3D printed surface texturing on the tribo-charging process of polymer slabs in conformal contact | Request PDF, in: ResearchGate, n.d. https://doi.org/10.1109/IAS54024.2023.10406393.
[43] N. Li, L. Ma, X. Xu, J. Luo, Influence of "Seebeck effect" on charge transfer between two friction surfaces, Tribol. Int. 161 (2021) 107060. https://doi.org/10.1016/j.triboint.2021.107060.
[44] Q. Li, W. Liu, H. Yang, W. He, L. Long, M. Wu, X. Zhang, Y. Xi, C. Hu, Z.L. Wang, Ultra-stability high-voltage triboelectric nanogenerator designed by ternary dielectric triboelectrification with partial soft-contact and non-contact mode, Nano Energy 90 (2021) 106585. https://doi.org/10.1016/j.nanoen.2021.106585.
[45] W. Li, L. Ma, X. Xu, J. Luo, Bidirectional electron transfer in Triboelectrification caused by friction-induced change in surface electronic structure, Nano Energy 114 (2023) 108667. https://doi.org/10.1016/j.nanoen.2023.108667.
[46] B. Neagoe, H.-N. Teodorescu, Y. Prawatya, L. Dascalescu, T. Zeghloul, Experimental bench for studying the relation between the dynamic characteristics of the frictional motion and the electric potential at the surface of polymer slabs in sliding conformal contact, Tribol. Int. 111 (2017) 107–115. https://doi.org/10.1016/j.triboint.2017.03.006.
[47] G.S.P. Castle, Contact charging between insulators, J. Electrost. 40–41 (1997) 13–20. https://doi.org/10.1016/S0304-3886(97)00009-0.
[48] M. Loos, Chapter 2 - Composites, in: M. Loos (Ed.), Carbon Nanotube Reinf. Compos., William Andrew Publishing, Oxford, 2015: pp. 37–72. https://doi.org/10.1016/B978-1-4557-3195-4.00002-3.
[49] K. Babooram, Chapter 1 - Brief overview of polymer science, in: R. Narain (Ed.), Polym. Sci. Nanotechnol., Elsevier, 2020: pp. 3–12. https://doi.org/10.1016/B978-0-12-816806-6.00001-7.
[50] N.K. Myshkin, M.I. Petrokovets, A.V. Kovalev, Tribology of polymers: Adhesion, friction, wear, and mass-transfer, Tribol. Int. 38 (2005) 910–921. https://doi.org/10.1016/j.triboint.2005.07.016.
[51] C. Sun, Y. Wang, M.D. McMurtrey, N.D. Jerred, F. Liou, J. Li, Additive manufacturing for energy: A review, Appl. Energy 282 (2021) 116041. https://doi.org/10.1016/j.apenergy.2020.116041.
[52] R. Aziz, M.I. Ul Haq, A. Raina, Effect of surface texturing on friction behaviour of 3D printed polylactic acid (PLA), Polym. Test. 85 (2020) 106434. https://doi.org/10.1016/j.polymertesting.2020.106434.